Angular Distribution of the Neutron Field and Energy Spectra in the Wendelstein-7-X hall

F. Herrnegger *, R. Burhenn, J. Sallander, J. Junker, A. Weller

Max-Planck-Institut für Plasmaphysik, EURATOM-Association
D-85748 Garching b. München, Germany
* email: franz.herrnegger@ipp-garching.mpg.de

1. Introduction

The knowledge of the neutron spectra and of their dependence along the toroidal angle φ of the Wendelstein-7-X torus is of importance and is analyzed by using the MCNP transport code. The present report shows that the dependence of the total neutron flux on φ is visible up to distances of approximately 400 cm from the neutron source. Outside of that distance the toroidal variation is negligible and only the radial distance from the neutron source matters.

The modeling of the Wendelstein-7-X torus is described in Ref.1, 2 and is illustrated by the Figs.1,2 in a cartesian coordinate system. Figs.1 shows horizontal cuts through the torus at planes $z = 0,\ 81,\ 150\ [cm]$. A quarter of the complete torus is shown which represents one complete and a quarter of a field period. Each of the five field periods is divided into 10 sections along the toroidal angle φ which is measured from the positive x-axis; R, φ, z are cylindrical coordinates.

The location of the point detectors is indicated by the outermost circle at R=850 cm. The concept of a measurement system for the neutron detection assumes five cylindrical detector boxes at (R=850 cm, z=150 cm) which are uniformly distributed along that circle; the diameter of the cylindrical boxes is 100 cm.

The torus arrangement (i.e. 50 modular field coils, 20 auxiliary field coils, cryostat enclosing all the coils, etc.) is modeled as circular torus with circular cross section and subdivided into cells which are individually bounded by a set of surfaces, i.e. the only cell bounding surfaces are planes and cylinders. The 50 twisted modular field coils (mf) and the 20 tilted auxiliary field coils (af) are all simplified by plane circular coils, the orientation of which is perpendicular to the equatorial plane.

The magnetic axis is assumed as a plane circle with major radius of R=550 cm. The divertor structure and their extension in toroidal direction is visible on the cut at z=81 cm and consists of 5 pieces. A similar divertor structure is assumed for the negative z-region (z<0) but shifted by $\Delta\varphi = 36^o$ (half of a field period) in toroidal direction in accordance with the stellarator symmetry. One complete field period extends from $\varphi = 0^o$ to $\varphi = 72^o$. The present geometrical model of the torus and the hall assumes a cylindrical wall which extends from R=1770 cm to R=1950 cm (borated concrete wall, not visible on Fig.1). The clear height of the hall is 24 m.

The experimental hall has in reality a rectangular shape. The thickness of the walls is 1.8 m; The thickness of the roof and the ground floor is 1.2 m. Injector boxes for neutral particles and other equipments outside the experimental device but inside the hall are not included in the present model but it will be implemented in the future.

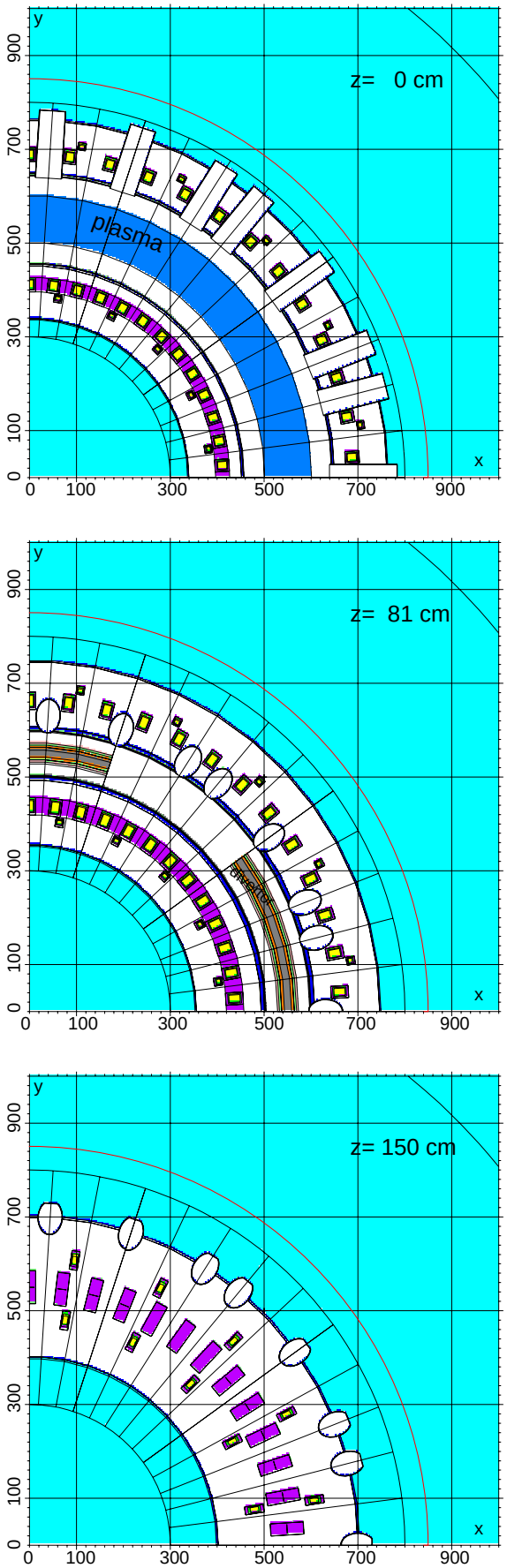

Fig.1. Cut through the torus at various horizontal planes: a quarter of the torus is shown.

The almost monoenergetic neutrons produced in the plasma region will interact with the surrounding material. These collisions lead to scattering, energy loss and absorption of the neutrons. This fairly complex transport problem has been studied in the literature by applying different approaches. One approach uses deterministic methods which leads to the problem of solving a singular integro-differential equation. This approach is well suitable for one-dimensional plane, cylindrical and spherical symmetric geometries. Examples for tokamaks with circular as well as with D-shaped cross sections are given in Ref.5,6. The stellarator geometry is more complex and does not fit into this approach.

One other method to solve the neutron transport problem for more general non-symmetric geometries such as stellarators and for the full energy distribution of the neutrons is to apply statistical methods by using random numbers to determine the outcome of each individual collision. The probability distributions are randomly sampled at each event using the appropriate cross-sections for energy loss, scattering and absorption. For this study the cross sections for stainles steel, copper, solder, molybdenum (divertor), superconductor (Al, Mg, Si, Ti, Cr, Cu, Nb), argon, air are needed.

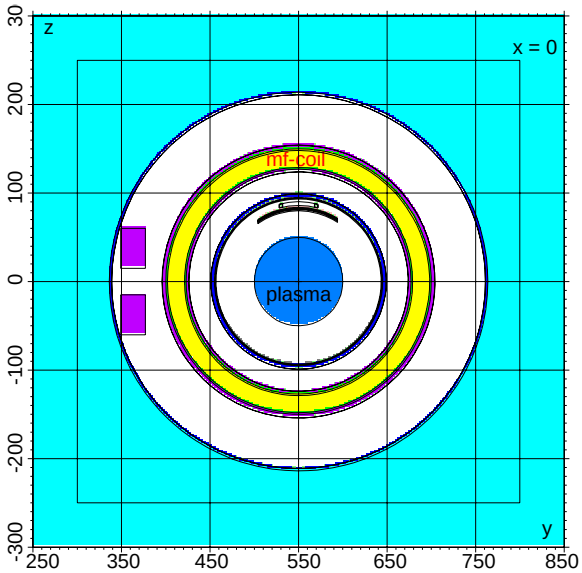

Fig.2. Cut through the torus at the vertical plane x=0.

This is provided by the Monte Carlo Neutron Particle code MCNP [Ref.3] together with the extensive ENDF-B-VI library [Ref.4] for the cross section data. Starting from an arbitrary three-dimensional neutron source, the neutron flux and the energy spectrum can be evaluated everywhere in geometrical space.

2. Results

The two fusion reactions D(d,n) ^{3}He and D(d,p) ^{3}T have about the same probability, the tritons are produced at 1 MeV, the neutrons at 2.46 MeV. The tritons can react with the deuterons D(t,n) ^{4}He and produce neutrons at 14 MeV at a very low rate in case of Wendelstein 7-X because the triton density is very low compared to the deuterium density. Because of the same reasons, T(t,2n)^{4}He and D(t,n)^{4}He reactions are not considered here.
The subsequent figures show the neutron flux normalized to the energy interval of 1 MeV and unit area of 1 cm^2 at various positions of a point detector and of a ring detector.

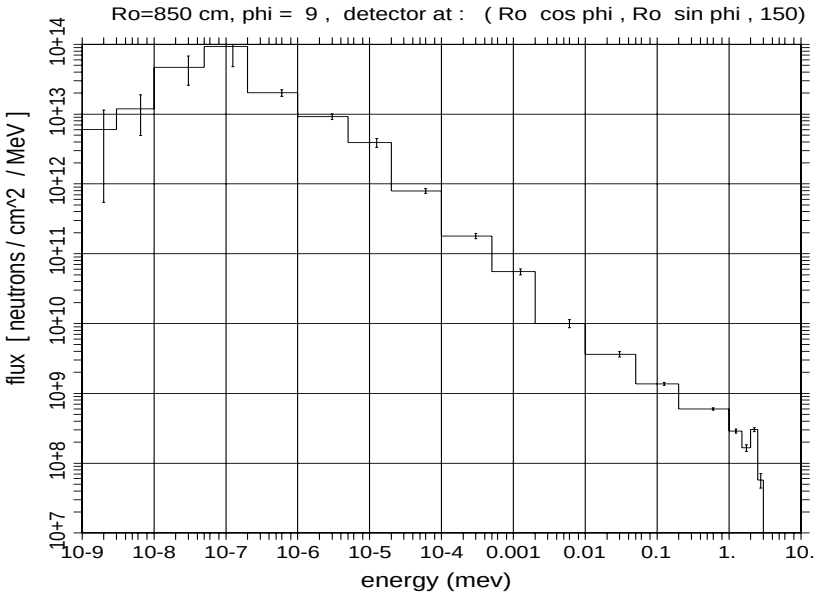

The ring source for the neutrons is located at R=550 cm, z=0 cm (cylindrical coordinates with origin at R=0, z=0) and produces Q=10^{16} neutrons per second with a Gaussian energy distribution (full half-width 0.2 MeV).

Fig.3. Neutron flux measured by the point detector at $\varphi = 9^o$.

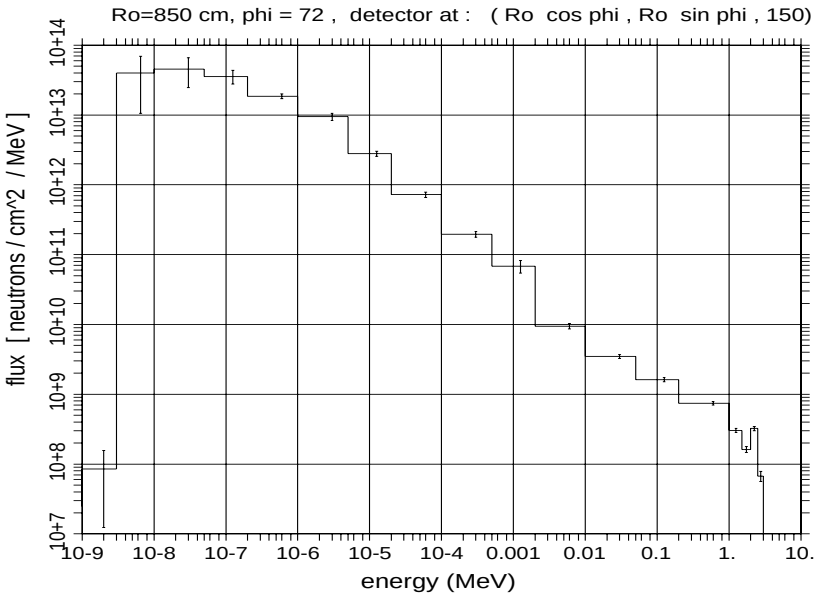

Fig.4. Neutron flux measured by the point detector at $\varphi = 72^o$. Changes of the spectrum occur at thermal energies around 10^{-8} MeV.

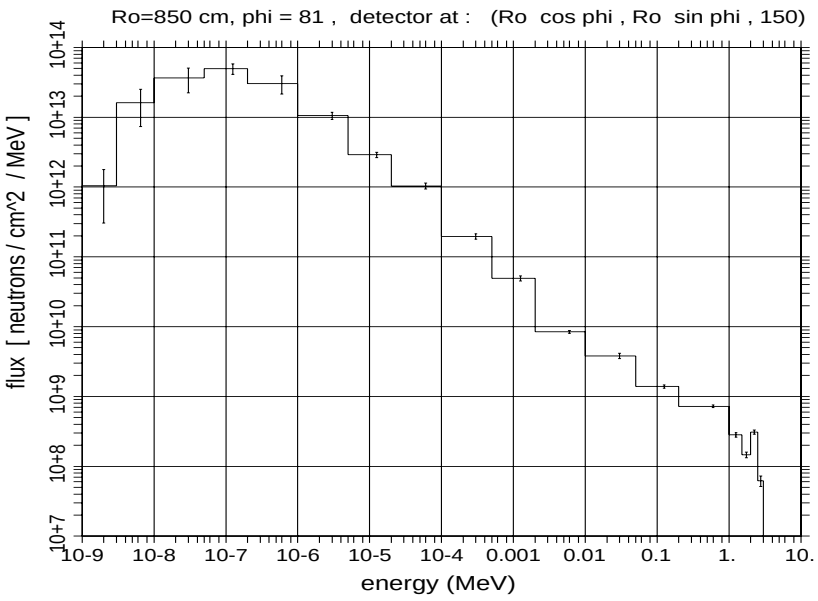

Fig.5. Neutron flux measured by the point detector at $\varphi = 81^o$.

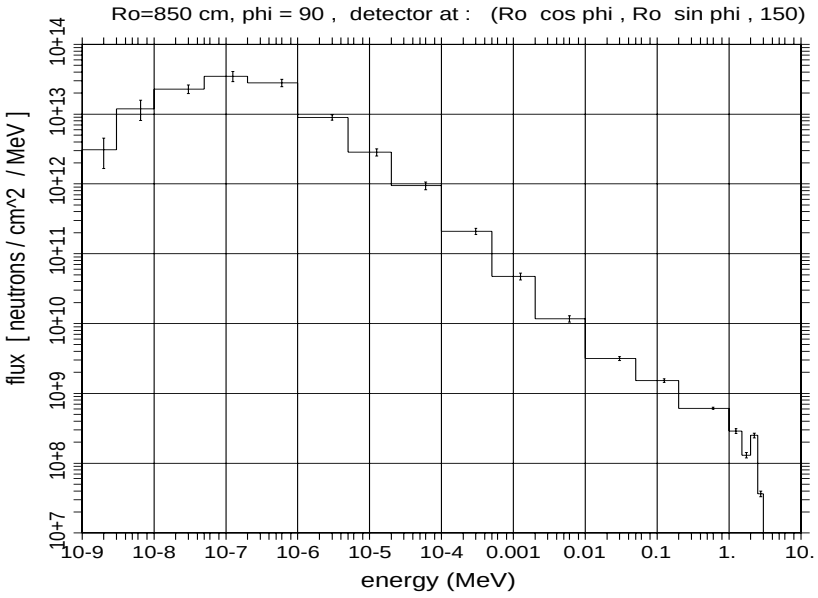

Fig.6. Neutron flux measured by the point detector at $\varphi = 90^o$.

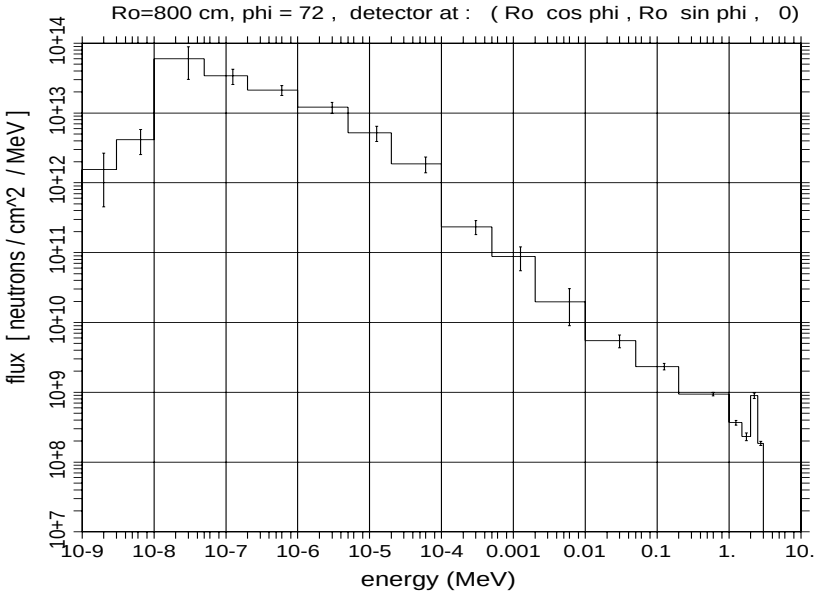

Fig.7. Neutron flux measured by the point detector at $\varphi = 72^o$ and R=800 cm i.e. more close to the torus structure. The number of neutrons is increased at high energy around 2 MeV.

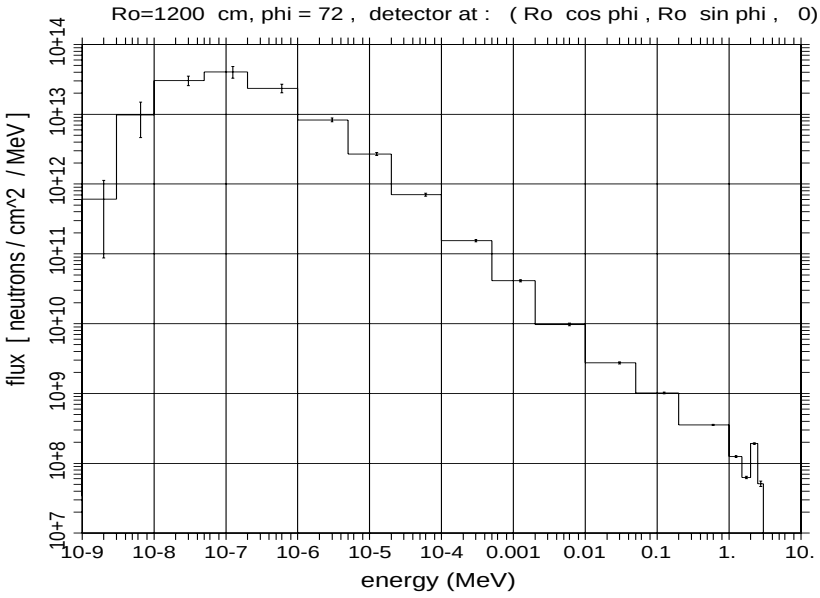

Fig.8. Neutron flux measured by the point detector at $\varphi = 72^o$

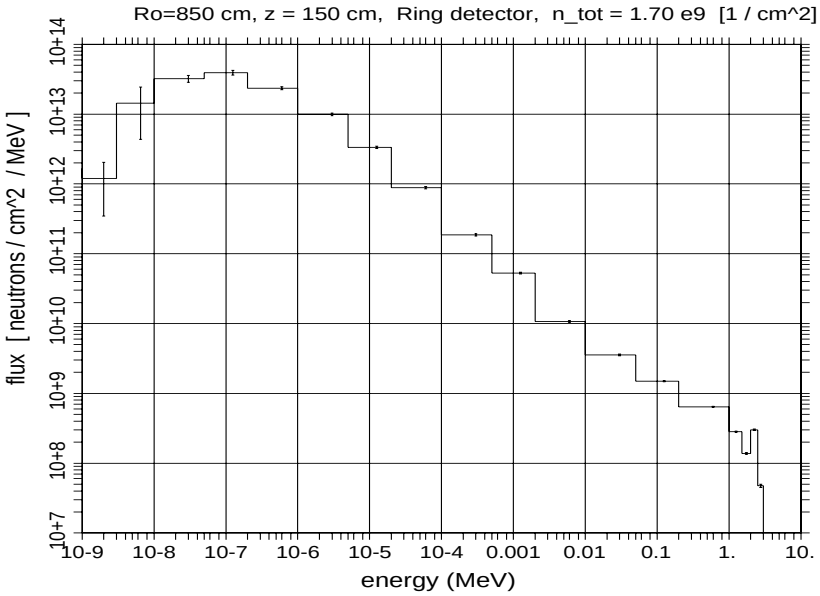

Fig.9. Neutron flux measured by the ring detector at R=850 cm, z=150 cm. The total neutron flux as given here is approximately the same as the average of the values given in Fig.13 for the case of z=150 cm.

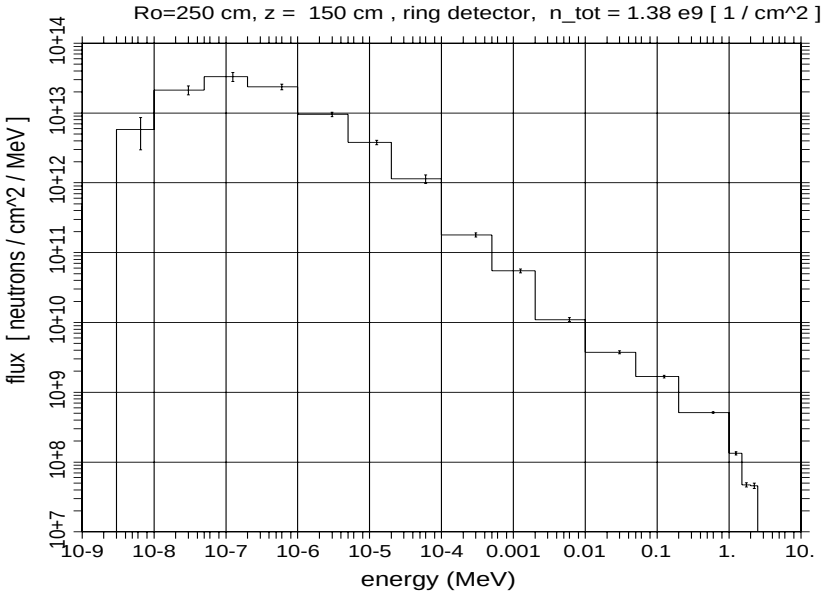

Fig.10. Neutron flux measured by the ring detector at R=250 cm, z=150 cm i.e. inboard site of the torus. The total number of neutrons per cm^2 is smaller than in the case of Fig.9. The neutron flux is considerably changed at an energy around 2 MeV.

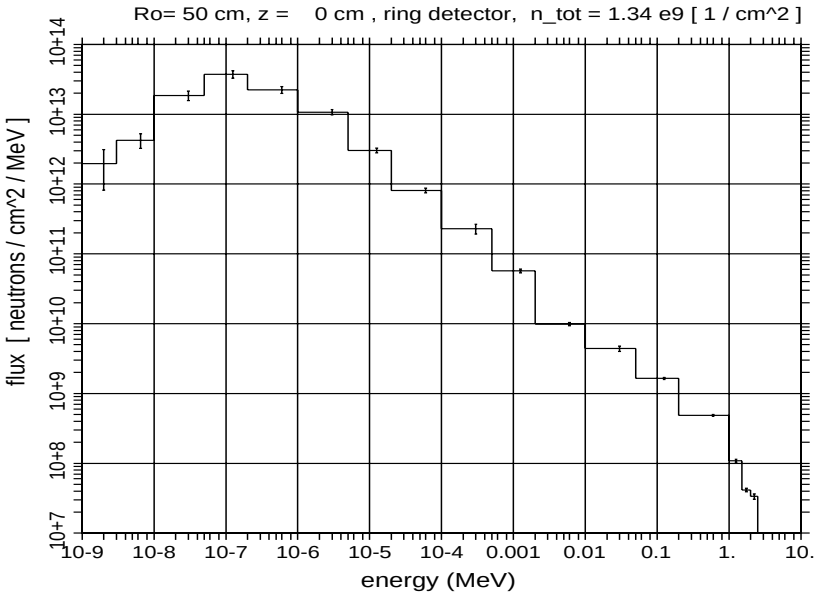

Fig.11. Neutron flux measured by a ring detector located close to the origin. The flux of neutrons with energies around 1 MeV is considerably reduced.

The total neutron flux is shown in Fig.12 as function of φ evaluated by a point detector at various vertical position. The effect of the periodic structure of the device on that quantity can be observed. At a height of |z| > 300 cm there is no significant dependence on φ.

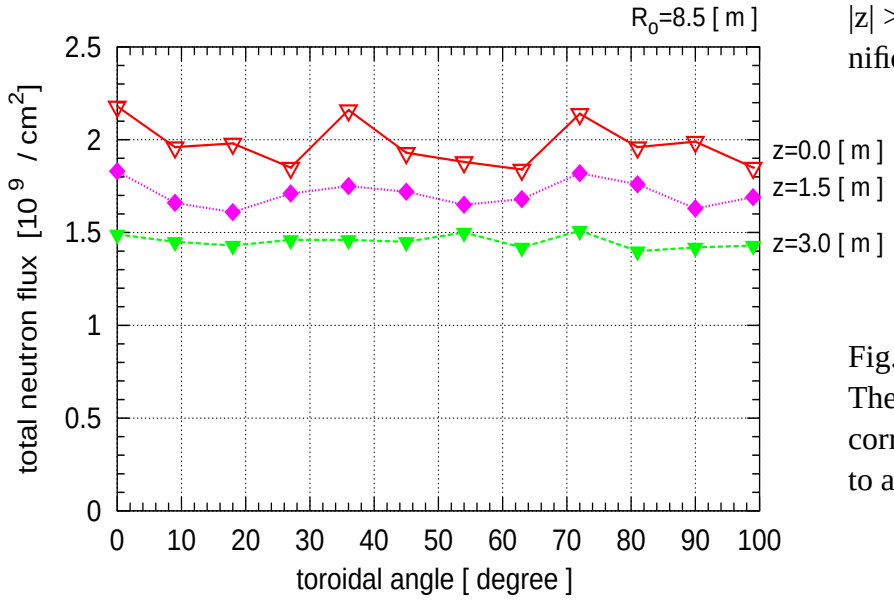

Fig. 12. Total neutron flux. The interval of 10 degree corresponds approximately to a length of 1.5 m.

References

[1] J. Junker and A. Weller, Neutrons at W7-X, IPP Report, Max-Planck-Institut für Plasmaphysik, Garching, IPP-2/341, October 1998.

[2] F. Herrnegger, J. Junker, A. Weller, H. Wobig, Neutron Field in the Wendelstein 7-X Hall, Fusion Engineering and Design **66-68** (2003) 849-853.

[3] J.F. Briesmeister (Ed.), MCNP - A General Monte Carlo N-Particle Transport Code, Version 4B, Los Alamos National Laboratory, LA-12625-M, March 1997.

[4] Harl'O M. Fisher, A Nuclear Cross Section Data Handbook, Los Alamos National Laboratory, LA-11711-M, December 1989.

[5] G. Fieg, Monte Carlo Calculations with the MCNP Code for Investigations of Neutrons and Photon Transport at the ASDEX Upgrade Tokamak, Report KfK 4851 (1991) (Kernforschungszentrum Karlsruhe).

[6] U. Fischer, Die neutronenphysikalische Behandlung eines (d,t)-Fusionsreaktors nach dem Tokamakprinzip (NET), Report KfK 4790 (1990) (Kernforschungszentrum Karlsruhe).